Highly adhesive hydroxyapatite coatings on titanium alloy formed by ion beam assisted deposition

F. Z. CUI*, Z. S. LUO, Q. L. FENG
Department of Materials Science and Engineering, Tsinghua University, Beijing 100 084, People's Republic of China

A compact crystalline hydroxyapatite coating on Ti–6Al–4V substrate with an atomic intermixed coating/substrate interface about 27 nm in width was synthesized by ion beam assisted deposition (IBAD) and a following post-treatment. The coating after post-treatment was identified by X-ray diffraction as crystalline hydroxyapatite. The interface between coatings and substrates was studied by Auger electron spectroscopy. The adhesive strength between coatings and substrates was measured by scratch tester. The results showed that the adhesive strength of IBAD coatings is nearly twice that of ion beam sputtered coatings. The study also showed that coatings prepared by IBAD eliminated the interfacial deficiencies existing in plasma-sprayed coatings.

1. Introduction

Hydroxyapatite (HA) coatings on titanium alloy have been widely studied, and have been used extensively in orthopaedic prostheses because of their biocompatability and ability to form a chemical bond with bone. There are several methods to make such coatings, among which plasma spraying is the most frequently used [1, 2]. However, long-term clinical follow-up has demonstrated that there are significant deficiencies in the plasma-sprayed HA coatings, which leads to limited longevity of replacement devices, with shorter life spans occurring in young, active individuals. The main problem with plasma-sprayed HA coatings is the limited strength of the coating–metal substrate interface and the limited cohesive strength of the coatings. In order to produce more permanent bone-bonding calcium phosphate coatings, ion beam assisted deposition (IBAD) was used in the present research. IBAD is known [3, 4] to provide bombardment with energetic ions during deposition, so that a wide atomic intermixed zone can be set up, thus giving strong adhesion of the coating to the substrate. Ohtsuka *et al.* first used 50 keV Ca^+ implantation into Ti, followed by Ca^+ IBAD to form a HA coating on Ti substrate and obtained higher adhesive strength than when using conventional methods [5]. It has been demonstrated that Ca^+ implantation alone into Ti was unable to provide the bioactive surface [6]. In the present paper, we report results on the formation of highly adhesive hydroxyapatite coatings on titanium alloy using Ar^+ IBAD. For practical use, the latter method has some advantages.

2. Materials and methods

A polyfunctional IBAD system [7] has been used to synthesize coatings. The system is equipped with three broad-beam Kaufman ion sources, a rotatable water-cooled sample holder, and a rotatable target. In experiments, the base pressure of the chamber was below 3×10^{-4} Pa, the working pressure was about 1.8×10^{-2} Pa. Flat Ti–6Al–4V substrates were polished with 0.3 μm alumina powder and ultrasonically degreased in acetone and alcohol baths, each for 10 min. Prior to deposition, the substrate surfaces were cleaned by Ar^+ bombardment at 100 $\mu A/cm^2$ and 3 keV for 10 min. The target having 70% HA and 30% tricalcium phosphate ($Ca_3(PO_4)_2$, TCP) content was sputtered by 3.5 keV Ar^+, and the resulting coatings were simultaneously bombarded by another energetic Ar^+ beam. First, the bombardment energy of the Ar^+ beam was selected to be 30 keV to produce an atomic intermixed layer of coating and substrate. When the thickness of the intermixed layer approached the projection range of the 30 keV Ar^+, the bombardment energy was reduced to 200 eV to grow the coating and to reinforce the compactness. The substrate temperature measured during deposition was below 100 °C. In order to compare the characteristics of coatings prepared by IBAD, ion beam sputtering deposition (IBSD) was carried out to form calcium phosphate coatings. The cleaning and sputtering conditions used for IBSD were similar to those used for IBAD. Some specimens were subjected to the following post-treatment after deposition: first, annealed at 500 °C for 2 h and then immersed in deionized water for 72 h at room temperature.

*Author to whom all correspondence should be addressed.

0957–4530

The structure of the coatings was identified by X-ray diffraction (XRD) with Cuk$_\alpha$ radiation using a Rigaku D/max-RB diffractometer operated at 40 keV and 80 mA. The surface morphology of the coating was examined by scanning electron microscopy (SEM), model Hitachi S-450. The Ca/P ratio of the coatings was determined by energy dispersive spectroscopy (EDS). The composition across the interface between coatings and substrates was analysed by Auger electron spectroscopy (AES), model PE-PHI-610. The adhesive strength between coatings and substrates was measured by scratch tester (CSR-01 Rhesca).

3. Results and discussion

SEM observations showed that no cracks were present in both the as-deposited and post-treated coatings. The surface layer of the coatings was relatively dense and homogeneous in appearance.

We have investigated the structural evolution of the coatings during preparation. Fig. 1 shows XRD patterns from the specimens at several conditions. The XRD pattern (d) of the as-deposited coatings showed an amorphous structure, with the central position of the amorphous diffraction peak at around 30°. After post-treatment, the structure of the coatings transformed into crystalline phases, as seen in pattern (e). From this pattern, the dominant crystalline phase was identified to be HA, and trace contents of tetracalcium phosphate ($Ca_4P_2O_5$, TeCP) and TCP can also be detected. It is seen that thirteen diffraction peaks from the HA phase were indexed in the pattern. Composition analysis by EDS showed that the Ca/P ratio of the post-treated coating is between 1.63 and 1.70, being close to that of HA (1.67). This composition analysis is consistant with the above structural determination by XRD.

The composition profiles near the interface between coatings and substrates were investigated by AES. The coating thickness for AES analysis was controlled to be about 30 nm. Typical depth profiles of the specimens prepared by both IBSD and IBAD are presented in Fig. 2. From the depth profile, we can define the interfacial width as the region between 5% Ti and 5% Ca. The interfacial width of the specimens prepared by IBSD and IBAD were determined to be 17 nm and 42 nm, respectively. According to sputtering theory [8], the energy of the most sputtered particles from the target is less than 10 eV. Thus, the mean penetration depth of the sputtered particles into the substrate in IBSD is below 1 nm [9]. In other words, the interfacial width of the specimen prepared by IBSD is only 1–2 atomic layers. The discrepancy in the interfacial width between AES analysis and theoretical consideration can be attributed to the ion mixing effects induced by Ar^+ sputtering [10]: the error in AES analysis of interfacial width is about 15 nm. Subtracting the error induced by AES analysis, the actual interfacial width in the IBAD specimen is determined to be about 27 nm. Using Monte Carlo dynamics simulation [11],

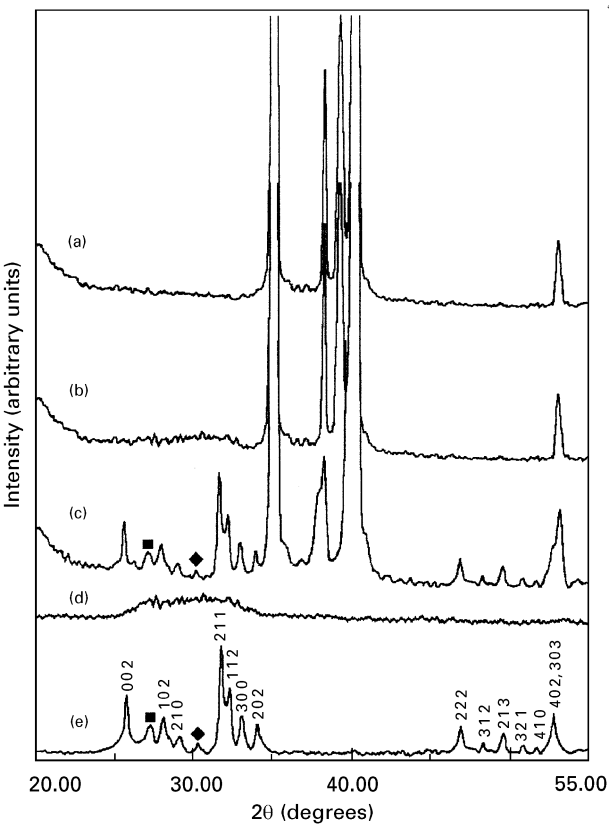

Figure 1 X-ray diffraction patterns from (a) Ti–6Al–4V substrate; (b) as-deposited coating; (c) post-treated coating; (d) and (e) were obtained from (b) and (c) by subtracting the substrate signals (■ TeCP, ◆ TCP).

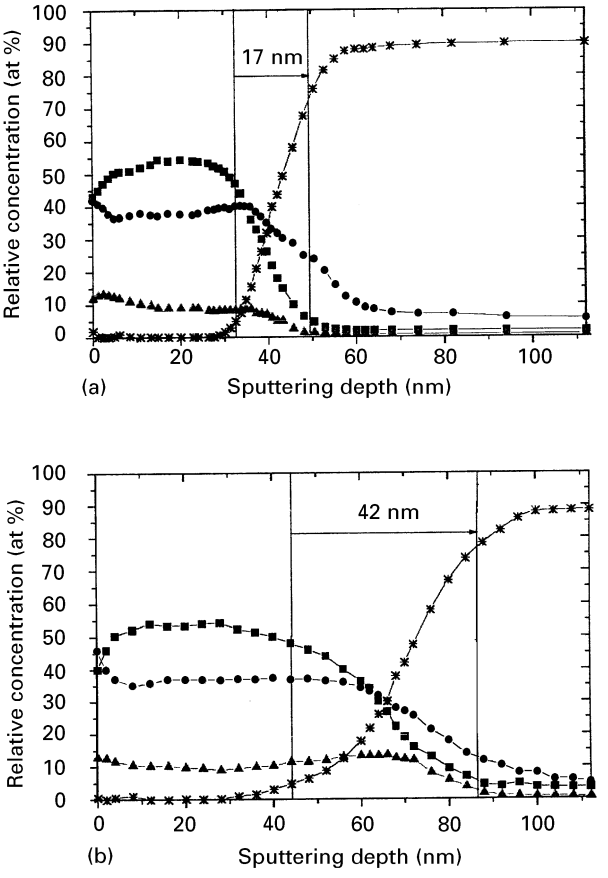

Figure 2 AES depth profiles of specimens prepared by (a) IBSD and (b) IBAD. The interfacial width in the specimens is indicated by arrows: ■ Ca; ● O; ▲ P; × Ti.

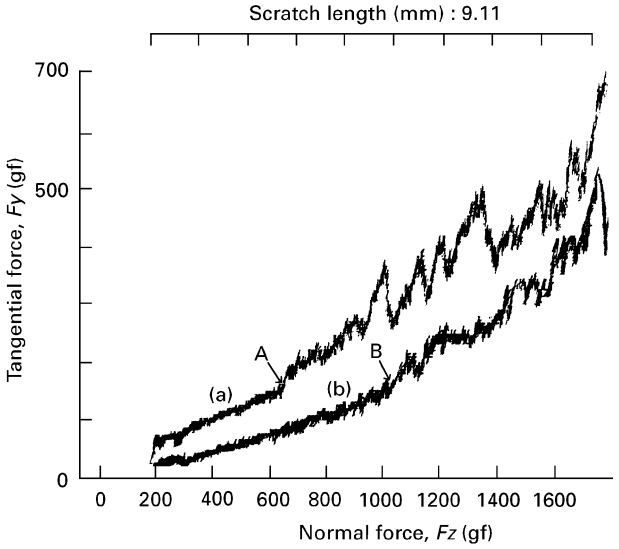

Figure 3 Fz–Fy curve of scratch test from specimen prepared by (a) IBSD and (b) IBAD. Arrows A and B indicate the points where coating removal first occurs. The critical load for IBSD is 660 gf and for IBAD is 1050 gf. The loading speed was 2 kg/min.

we have calculated that the interfacial width is 29 nm for the IBAD process. This coincides reasonably with the experimental results. It is worth mentioning that the O and P signals in the AES spectra deviated from the actual concentrations. It has been pointed out in previous studies on HA composition profile analysis by AES [12] that the relative Auger sensivity factors for the respective elements within HA may be different from those published in standard spectra.

The adhesive strength of the IBSD and IBAD coatings to the substrates was investigated by scratch tests. Fig. 3 shows typical Fz–Fy curves of scratch tests from specimens prepared by IBSD and IBAD. Arrows A and B indicate the points where coating removal from the substrate first occurs. Fz and Fy are the normal and tangential forces, respectively, affecting the diamond indenter during the test. Critical loads for the coatings prepared by IBSD and IBAD at a load speed of 2000 gf/min were determined to be 660 gf and 1050 gf, respectively. Thus the adhesive strength of the coatings prepared by IBAD is nearly twice that of the IBSD coatings.

It has been demonstrated that the adhesive strength of coatings prepared by IBSD is similar to that of plasma-sprayed coatings [13]. It can therefore be deduced from the above results that the adhesive strength of IBAD coatings is much higher than that of plasma-sprayed coatings. As we know, the main advantage of IBAD over other methods, e.g. IBSD or plasma spraying, is that there is a wide atomic intermixed zone at the coating/substrate interface [4, 5]. It is the intermixed zone that significantly contributes to the improvement of the adhesive strength. Thus the main deficiency existing in plasma-sprayed coatings can be effectively eliminated by using the IBAD method.

4. Conclusions

A compact crystalline HA coating with strong adhesive strength to Ti substrates has been obtained by using the method of IBAD. The adhesive strength is nearly twice that of IBSD coatings. As the interface produced by ISBD and plasma spraying is physically similar, the main interfacial deficiency existing in plasma-sprayed coatings can be eliminated by use of IBAD coatings.

Acknowledgements

The authors thank Dr X. M. He for his help with IBAD experiments. This work was in part supported by the National Natural Science Foundation of China and National 863 Project in Advanced Techniques in China.

References

1. H. AOKI, "Science and medical application of hydroxyapaptite" (Takayama Press, Tokyo, 1991).
2. R. G. T. GEESINK and M. T. MANLEY, "Hydroxyapatite coatings in orthopaedic surgery" (Raven Press, New York, 1993).
3. R. A. KANT, B. D. SARTWELL, I. L. SINGER and R. G. VARDIMIZE, *Nucl. Instrum. Meth.* **B7/8** (1987) 915.
4. F. A. SMIDT, *Int. Mater. Rev.* **35** (1990) 61.
5. Y. OHTSUKA, M. MATSUURA, N. CHIDA, M. YOSHINARI, T. SUMII and T. DERAND, *Surf. Coatings Technol.* **65** (1994) 224.
6. M. SPECTOR, Private communication.
7. X. M. HE, W. Z. LI, H. D. LI and Y. FAN, *Nucl. Instrum. Meth.* **B82** (1993) 528.
8. Y. OHMURA, Y. MATSUSHITA and M. KASHIWAGI, *Jpn. J. Appl. Phys.* **21** (1982) 152.
9. H. F. WINTERS and E. TAGLAUER, *Phys. Rev.* **B35** (1987) 2174.
10. L. C. FELDMAN and J. W. MAYER, "Fundamentals of surface and thin film analysis" (Elsevier Science, 1986).
11. F. Z. CUI, H. D. LI and J. P. ZHANG, *Nucl. Instrum. Meth.* **B21** (1987) 478.
12. W. V. RAEMDONK, P. DUCHEYNE and P. D. MEESTER, *J. Amer. Ceram. Soc.* **67** (1984) 381.
13. J. L. ONG, L. C. LUCAS, W. R. LACEFIELD and E. D. RIGNEY, *Biomaterials* **13** (1992) 249.

Received 5 August
and accepted 18 September 1996